



A fused soil moisture product integrating linear fusion method and error characteristics approach

Anuj Singh, C.T. Dhanya & M. Saharia

To cite this article: Anuj Singh, C.T. Dhanya & M. Saharia (05 Apr 2026): A fused soil moisture product integrating linear fusion method and error characteristics approach, International Journal of Remote Sensing, DOI: [10.1080/01431161.2026.2653239](https://doi.org/10.1080/01431161.2026.2653239)

To link to this article: <https://doi.org/10.1080/01431161.2026.2653239>



View supplementary material [↗](#)



Published online: 05 Apr 2026.



Submit your article to this journal [↗](#)



Article views: 41



View related articles [↗](#)



View Crossmark data [↗](#)



A fused soil moisture product integrating linear fusion method and error characteristics approach

Anuj Singh, C.T. Dhanya and M. Saharia

Department of Civil Engineering, Indian Institute of Technology Delhi, New Delhi, India

ABSTRACT

Soil moisture is critical for understanding the hydrological cycle and managing climatic extremes such as floods and droughts. This study evaluates the accuracy of satellite-derived soil moisture estimates from remote sensing satellite products Soil Moisture Active Passive (SMAP), Soil Moisture and Ocean Salinity (SMOS), and Advanced Microwave Scanning Radiometer-2 (AMSR-2) in the absence of ground observations. A selective fusion algorithm is introduced that enhances accuracy by fusing data only in regions where it improves the precision of soil moisture estimates, rather than applying a uniform fusion approach across all regions. Using Extended Triple Collocation (ETC) analysis, the error characteristics of individual satellite products are assessed across spatial, temporal, and meteorological aspects. Additionally, Mutual Information (MI) analysis with precipitation data quantifies the information content of each product to validate their effectiveness. Our results demonstrate that SMAP consistently exhibits the lowest error characteristics and highest information content. Notably, AMSR-2 shows superior performance in hot desert and semi-arid regions, highlighting the need for a spatially adaptive fused soil moisture product. An integrated fusion algorithm, guided by a decision map based on these analyses, optimizes the selection of soil moisture products across India's diverse regions. This decision map revealed the highest spatial coverage by SMAP (62.5%), followed by AMSR-2 (25.7%) and SMOS (5.6%), with the remainder attributed to various combinations of products that provide superior soil moisture estimates in specific contexts. This modified fusion approach is implemented using a Linear Weight Fusion (LWF) technique, significantly enhancing the reliability of the resultant soil moisture product, particularly evident from its validation against data from three in-situ stations. The integrated approach not only refines the accuracy of satellite-derived soil moisture data but also provides a robust framework for enhancing hydrological model predictions, especially in drought monitoring.

HIGHLIGHTS

- Performed Extended Triple Collocation (ETC) and Mutual Information (MI) analysis to evaluate and merge SMAP, AMSR-

ARTICLE HISTORY

Received 21 May 2025

Accepted 20 March 2026

KEYWORDS

Satellite soil moisture; triple collocation; SMAP; mutual information; linear weight fusion

2, and SMOS satellite-derived soil moisture estimates across India.

- Demonstrated that each product shows better results over a certain region, emphasizing the importance of region-specific product suitability.
- Developed a fused soil moisture dataset using ETC and MI informed Linear Weight Fusion (LWF) algorithm, enhancing spatial and temporal consistency over data-sparse Indian regions.
- Validated the fused product against in-situ observations (COSMOS) and model-based (GLEAM and ERA5) datasets.
- Proposed framework holds potential for integration of resulting product with land surface models for early-warning systems, water resource management, and climate impact studies under changing climate scenarios.

1. Introduction

Soil moisture is a key variable in the hydrological cycle which affects climate and weather patterns, by playing a vital role in regulating land-atmosphere interactions and influencing energy and water fluxes (Entekhabi 1995). Although it constitutes only ~0.15% of Earth's freshwater, soil moisture significantly impacts ecological and agricultural systems by governing plant growth, evapotranspiration, and the spatio-temporal availability of water (Dingman and Dingman 2015; Rodriguez-Iturbe 2000). Its variability is closely linked to climatic factors such as temperature and precipitation, and affects key land surface processes including energy partitioning, runoff generation, and vegetation dynamics (Huszár et al. 1999; Porporato, Daly, and Rodriguez-Iturbe 2004; Riley and Shen 2014; Rosenbaum et al. 2012; Si et al. 2023; Wang et al. 2019). Furthermore, soil moisture monitoring is essential for predicting extreme events like droughts and floods, and for assessing plant stress and crop yield responses under changing climate conditions (Erdenebat and Sato 2018; Ajaz et al., 2018; Vogel, Zscheischler, and Seneviratne 2018; Whan et al. 2015; Xu et al. 2020).

Soil moisture is typically monitored through in-situ measurements such as gravimetric method, neutron probes, electromagnetic methods, etc., and through remote sensing measurements such as microwave remote sensing, that ensures large-scale measurements (Engman and Chauhan 1995; Jackson, Schmugge, and Engman 1996; Schmugge, Jackson, and McKim 1980). Realizing the need for a well-distributed soils moisture network across the world, in 2009, International Soil Moisture Network (ISMN) was established to validate and calibrate model and satellite-based data using a global in-situ soil moisture database comprising 3202 stations across 80 networks (<https://ismn.earth/en/dataviewer/>). However, the sparse distribution of these stations posed challenges in validating the data at continental-scales, particularly in regions like India where stations are few (W. A. Dorigo et al. 2011, 2013). The Indian COSMOS Network (ICON), using Cosmic Ray Neutron Probe (CRNP) technology, offers data from merely seven major stations and therefore lacks sufficient coverage for comprehensive validation across diverse climatic zones in India (Upadhyaya et al. 2021; Zreda et al. 2012).

Due to the limited spatiotemporal coverage of in-situ data, satellite-derived soil moisture datasets are increasingly used for hydrological and climate studies (Nouri and Homaei 2021). Missions such as Soil Moisture Active Passive (SMAP) (Entekhabi et al.

2010) and Soil Moisture and Ocean Salinity (SMOS) (Al Bitar et al. 2017), deploy different algorithms to convert passive microwave data into soil moisture, resulting into diverse mean, variance, and skewness in these products. These have been already applied to soil moisture products like Advanced Microwave Scanning Radiometer (AMSR)-E (Jackson 1993; Jones et al. 2009; Koike et al. 2004; Njoku, Jackson, and Chan 2004; Owe, de Jeu, and Walker 2001). This use of multiple algorithms to retrieve soil moisture data makes it difficult to determine which technique is most accurate.

In the absence of reliable ground truth, statistical approaches such as Triple Collocation Analysis (TCA) (Stoffelen 1998) are widely employed to assess satellite soil moisture product performance (Cheema, Bastiaanssen, and Rutten 2011; W. A. Dorigo et al. 2010; Draper et al. 2013; Scipal et al. 2010, 2008; Xu et al. 2021). Additionally, several studies leveraged the relationship between soil moisture and precipitation variability to evaluate satellite soil moisture accuracy; for example, Tuttle and Salvucci (2014), Salvucci (2001), Karthikeyan and Kumar (2016), Huggannavar and Indu (2020), Krishnan, Pradhan, and Indu (2022) deployed variety of approaches including Mutual Information (MI), water balance method, influence of land use and elevation on satellite-derived soil moisture etc.

Beyond evaluation, many studies attempted to fuse different datasets with diverse characteristics to generate merged soil moisture products through various fusion approaches like Linear Weight Fusion (LWF), Non-Linear Weight Fusion, Artificial Neural Network (ANN), Copula-based data fusion, Multiple Linear Regression, and Least Square Method (Das et al. 2016; Kim et al. 2015; Liu et al. 2012; Santi et al. 2018; Xie et al. 2022). More recent advances have emphasized the importance of accounting for spatially and temporally varying error characteristics during fusion. For example, Gruber et al. (2017) introduced a triple-collocation based merging scheme that adapts weights according to regional error statistics, Zhou et al. (2021) proposed a two-dimensional (time-space) triple collocation framework to address non-stationary error structures, Peng et al. (2021) demonstrated the integration of model simulations and satellite products for high-resolution soil moisture estimates in Great Britain, and Zhao et al., (2024) compared traditional triple collocation techniques with deep learning approaches such as Long Short Term Memory (LSTM) network for adaptive soil moisture fusion. Collectively, these studies highlight the necessity of spatially adaptive schemes to improve fused products. Therefore, understanding and incorporating spatially varying error structures into the fusion framework is essential for improving soil moisture estimates.

Addressing these gaps, in this study we aim to analyse the error structure of the widely used soil moisture products such as SMAP, AMSR-2, and SMOS, by performing Extended Triple Collocation (ETC) analysis (McColl et al. 2014), followed by a validation of these products using a MI analysis to explicitly evaluate and optimize multi-sensor fusion across the highly heterogeneous hydro-climatic regions of India, where the absence of dense in-situ observations presents additional challenges. Further, we propose a novel stepwise fusion algorithm considering the spatial error characteristics to obtain a merged soil product with minimized error characteristics.

The sections of the study are structured as follows. Section 2 describes the study area and data used in this study. The methodology used for a comprehensive evaluation of soil moisture datasets is outlined in Section 3. In Section 4, we discuss the ETC and MI analysis, followed by fusion of the soil moisture products based on the decision map and the validation of newly formed soil moisture products. The study concludes with Section 5, elaborating the conclusions drawn from this study and the implications of the findings.

2. Study area and data used

We selected the Indian region, to demonstrate the proposed methodology, due to its diverse hydrometeorological characteristics. The dependency on monsoon-fed agriculture in India makes the study of soil moisture dynamics particularly vital. The region's agriculture heavily relies on accurate soil moisture data to optimize irrigation practices, enhance crop yields, and refine the forecasting accuracy of climatic extremes through hydrological models. The study utilizes Köppen-Geiger climatic classification map to analyse and visually depict the spatial variability of results across India. The Köppen-Geiger classification map is derived using three air temperature (WorldClim V1 and V2, CHELSA V1.2) and four precipitation (WorldClim V1 and V2, CHELSA V1.2, and CHPClim V1) climatic datasets (Beck et al. 2018). For Indian region, six major climatic zones constitute for more than 90% among all the climate types which specifically includes Am (Tropical Monsoon Climate), Aw (Tropical wet and dry or savanna climate), Cwa (Monsoon), BSh (Hot semi-arid climate), BWk (Cold desert climate), and BWh (Hot desert climate), as shown in Figure 1.

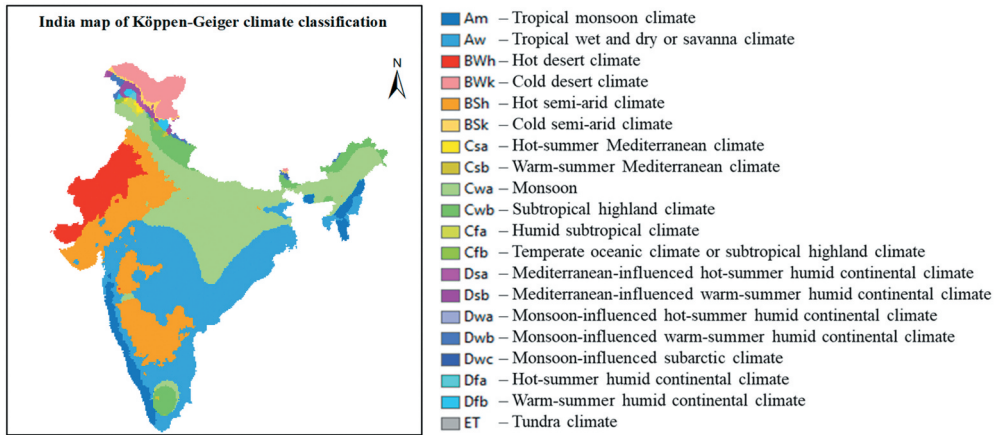


Figure 1. Köppen-Geiger climatic classification over India.

2.1. Soil moisture data

We considered three passive satellite retrieved soil moisture datasets, one model-based soil moisture product, and one active soil moisture product, as detailed in Table 1.

2.1.1. Passive soil moisture products

Level 3 passive satellite-retrieved soil moisture products, such as SMAP (Entekhabi et al. 2010; O'Neill et al. 2023), AMSR-2 (Teng and Parinussa, 2021) and SMOS (Al Bitar et al. 2017) are used, these products aggregate both ascending and descending overpasses into single daily composite product. All three products are in volumetric units, i.e. m^3/m^3 to facilitate comparative analysis. These satellites measure brightness temperature (T_b) in Kelvin [K], which is then converted into soil moisture values using distinct retrieval algorithms for each of the satellite. Among them, SMAP works in L-band (~ 1.41 GHz), AMSR-2 works in X-band and SMOS again works in L-band (~ 1.40 GHz). Despite SMAP and

Table 1. Different soil moisture products used in the study.

Sensor	Product	File naming convention	Time period	Band	Resolution	References
Passive	SMAP	L3_SM_P_E	2016–2019	L-band	9 km	Entekhabi et al. (2010)
	AMSR-2	LPRM_AMSR2_L3_DS_D	2016–2019	X-band	10 km	Teng and Parinussa (2021)
	SMOS	SM_RE07_MIR_CLF3SD	2016–2019	L-band	0.25°×0.25°	Al Bitar et al. (2017)
Model	GLDAS	GLDAS_CLSM025_DA1_D2.2	2016–2019		0.25°×0.25°	Rodell et al. (2004)
Active	ESA-ACTIVE	ESACCI_L3_ACT	2016–2019		0.25°×0.25°	W. Dorigo et al. (2017); Gruber et al. (2019); Preimesberger et al. (2021)

SMOS operating on similar frequencies, different algorithms deployed for retrieval makes them independent of each other. All the products are rescaled using bilinear interpolation considering SMAP L3 enhanced product as the reference.

2.1.2. Model-based soil moisture product

Global Land Data Assimilation System (GLDAS; Rodell et al. 2004), is an advanced land surface modelling and data assimilation system to produce highly accurate land surface states. GLDAS drives three main land surface models, i.e. Catchment Land Surface Model (CLSM), Noah, and Variable Infiltration Capacity (VIC). Each model utilizes unique sets of land surface characteristics and meteorological forcing datasets for simulation. For this study, GLDAS CLSM version 2.2 which integrates meteorological analysis fields obtained from the operational European Centre for Medium-Range Weather Forecast (ECMWF) Integrating Forecasting System is selected. We used the improved GLDAS products assimilated using the total terrestrial water anomalies data from Gravity Recovery And Climate Experiment (GRACE) satellite (Li et al. 2019), available from 2003 to 2023. The GLDAS CLSM daily soil moisture product is available at 0.25° spatial resolution. Soil moisture values in kg/m², are converted into volumetric units (m³/m³) using the corresponding soil depth layer to standardize the unit of measurement and facilitate comparison with other satellite-derived soil moisture products.

2.1.3. Active soil moisture product

We used European Space Agency-Climate Change Initiative (ESA-CCI) ACTIVE SM version 08.1, an active soil moisture product in this study. ESA-CCI offers three soil moisture datasets – passive, active, and combined: facilitating integration of new instruments during its operational phase. The active product integrates data from three active sensors, i.e. Active Microwave Instrument-WindScat (AMI-WS), ASCAT-A, and ASCAT-B (Advanced SCATterometer). These sensors estimate soil saturation degree (%) using the Soil Water Retrieval Package and reference backscattering coefficients for extreme dry and wet conditions (Zhu et al. 2019). To convert soil saturation to volumetric moisture (m³/m³), the product is scaled using global soil porosity data from the GLDAS-CLSM Soil Porosity Map (<https://ldas.gsfc.nasa.gov/gldas/soils>).

2.1.4. In-situ soil moisture data

This study used in-situ soil moisture daily data from 2016 to 2019 at three stations- Berambadi (BMB), Madahalli (MDH), and Singanallur (SGR), belonging to the Indian COSMOS Network (ICON) (Upadhyaya et al. 2021); for the fused product validation purpose. These stations use Cosmic Ray Neutron Probe (CRNP) sensors, which provide area-integrated soil moisture

estimates at the field scale and are primarily sensitive to near-surface soil layers. The ICON observations are independent of satellite-based soil moisture retrievals and serve as reference data for product evaluation.

2.2. Gridded precipitation dataset

We used the daily gridded rainfall dataset at $0.25^\circ \times 0.25^\circ$ resolution by India Meteorological Department (IMD) (Pai et al. 2014), prepared from daily rainfall records from around 6955 rain gauge stations over the country using Shepard method (Shepard 1968). The dataset is adjusted for orographic and other factors (Bharti et al. 2016; Pai et al. 2015), and ensures accurate representation of regional rainfall.

2.3. Irrigation data

Irrigation data through Global Map of Irrigation Areas – Version 5.0 (Siebert et al., 2013) at 5 arc minutes ($\sim 0.08^\circ$) resolution from Food and Agricultural Organization (FAO) is used. It utilizes annual data on irrigation water withdrawal (m³) gathered at national and sub-national levels and is disseminated through FAO's global water database, AQUASTAT (<https://www.fao.org/aquastat/en/>).

3. Methodology

All soil moisture datasets are rescaled to the SMAP spatial grids for the period 2016 to 2019. Considering the 2–3 days revisit times of SMAP/SMOS, this study period provided more than 400 collocated observations per pixels. Triplets of the soil moisture data are then formed, with passive-model-active combination, ensuring independence and zero error cross correlation among the datasets. The triplets formed, where the model and active data remain the same in all the three triplets, are structured as follows.

Triplet 1 - [SMAP – GLDAS – ESA_ACTIVE]

Triplet 2 - [AMSR_2 – GLDAS – ESA_ACTIVE]

Triplet 3 - [SMOS – GLDAS – ESA_ACTIVE]

Further, we developed a two-step analytical approach to evaluate the spatio-temporal error characteristics of these soil moisture products: (i) an Extended Triple Collocation (ETC) analysis to evaluate the spatio-temporal error characteristics of soil moisture products, and (ii) a validation using Mutual Information (MI) analysis between precipitation data and soil moisture products. ETC and MI analyses are performed to quantify the biases in soil moisture products and assess their dependencies on precipitation. The error variance from ETC and maximum information from MI for each grid are then considered in a decision map. This map suggests the best accurate soil moisture product at each grid point spatially over the entire domain at 9 km spatial resolution.

Further, comprehensive insights derived from these analyses are integrated into a fusion algorithm, while merging the datasets based on least error characteristics and highest information content of a specific dataset at a particular grid point. The overall methodology adopted in this study is shown as a flowchart in Figure 2.

A brief description of the methods adopted is provided below.

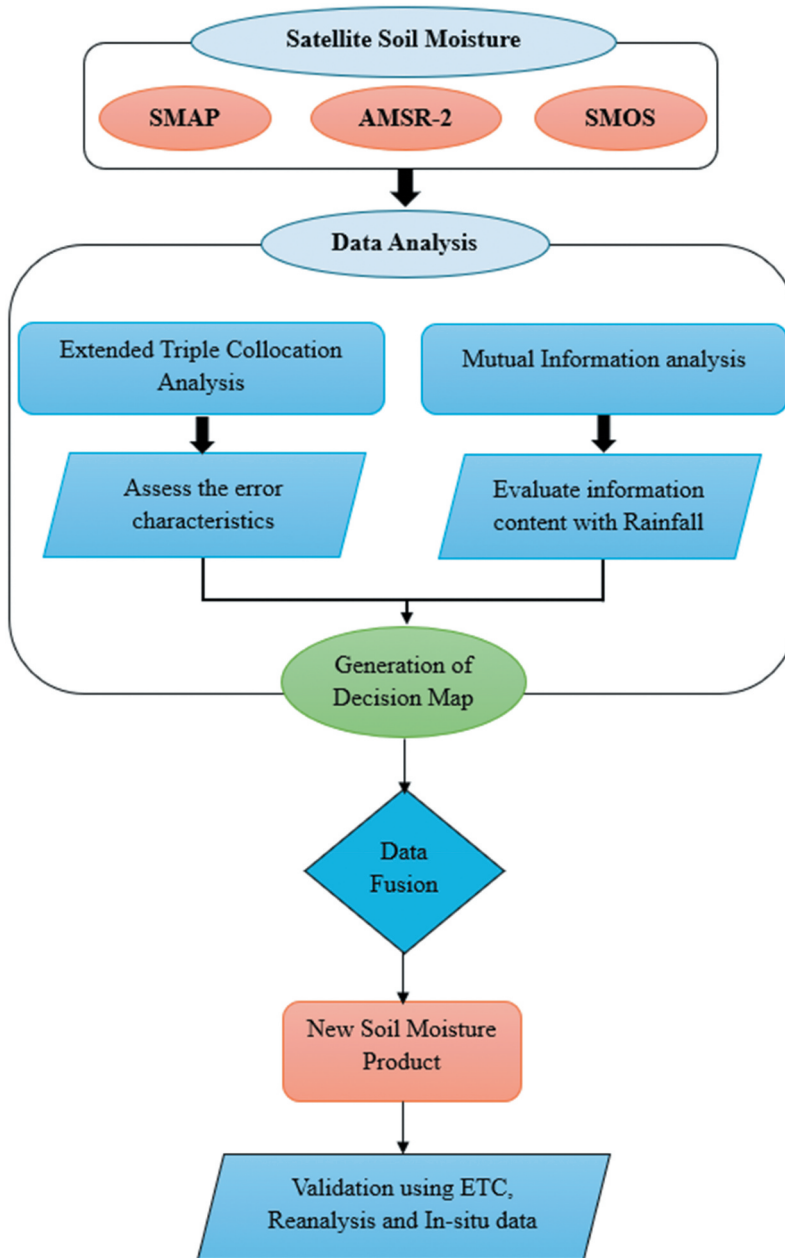


Figure 2. Workflow flowchart to generate new soil moisture product using ETC & MI analysis.

3.1. Extended triple collocation

TCA is a robust statistical method extensively applied to evaluate the accuracy of satellite-retrieved soil moisture products by quantifying systematic biases and random errors (Stoffelen and Vogelzang 2012), particularly in scenarios devoid of in-situ data. It has four major assumptions: the linearity between true and observed soil moisture,

orthogonality of errors relative to true soil moisture, zero error cross-correlations across independent datasets, and a minimum of 100 independent collocated observations are required in the sample to ensure the statistical robustness (Gruber et al. 2016; Scipal, Dorigo, and DeJeu 2010). These assumptions ensure that TCA can effectively isolate and quantify the random errors inherent in each dataset without any ground truth reference. The basic error model in TCA is given as:

$$SM = \alpha + \beta \cdot t + \varepsilon \quad (1)$$

which says that the retrieved soil moisture (SM , m^3/m^3) in each pixel is expressed as a linear relationship between true soil moisture (t , m^3/m^3) and random error (ε), where α and β are the coefficients that represent intercept and slope of the linear relationship between true and observed soil moisture. Further, the error variance, $\sigma_{\varepsilon_i}^2$ and correlation coefficients, $\rho_{(t, SM_i)}^2$ are expressed as:

$$\sigma_{\varepsilon_i}^2 = \begin{cases} Q_{11} - \frac{Q_{12}Q_{13}}{Q_{23}} \\ Q_{22} - \frac{Q_{21}Q_{23}}{Q_{13}} \\ Q_{33} - \frac{Q_{31}Q_{32}}{Q_{12}} \end{cases}, \text{ where } i \in [1, 2, 3] \quad \rho_{(t, SM_i)}^2 = \begin{cases} \frac{Q_{12}Q_{13}}{Q_{11}Q_{23}} \\ \frac{Q_{21}Q_{23}}{Q_{22}Q_{13}} \\ \frac{Q_{31}Q_{32}}{Q_{33}Q_{12}} \end{cases}, \text{ where } i \in [1, 2, 3] \quad (2)$$

where Q_{ij} denotes the covariance matrix and $(i, j) \in [1, 2, 3]$ signifies the three different passive products of each triplet. Lower error variance values depict more accurate and reliable dataset, whereas higher correlation coefficient implies stronger association between soil moisture measurements and dataset measurements.

3.2. Mutual information

MI analysis is utilized to quantify the non-linear dependencies between soil moisture and precipitation, as an indirect performance analysis of satellite soil moisture products. MI values help to assess the relationship between observed precipitation and soil moisture. A higher MI value suggests a strong relationship, indicating that the changes in soil moisture levels are closely associated with the changes in the precipitation. MI of two variables X and Y are expressed as,

$$MI(X, Y) = \sum_{x \in X} \sum_{y \in Y} p(x, y) \log \left[\frac{p(x, y)}{p(x)p(y)} \right] \quad (3)$$

where $p(x, y)$ denotes the joint probability distribution of variables X and Y , and $p(x)$ and $p(y)$ signify the marginal probability distribution of variables X and Y respectively.

3.3. Linear weight fusion

LWF technique is applied on those grids where fusion of soil moisture data is suggested by the decision map. When multiple datasets are required to fuse at a specific pixel, weights are

calculated (Xie et al. 2022) for each satellite soil moisture measurement. The weights are computed using the error variance (σ_ϵ^2) values from ETC method, as shown in Equation 4.

$$\begin{pmatrix} w_1 \\ w_2 \\ w_3 \end{pmatrix} = \begin{pmatrix} \frac{1/\sigma_{\epsilon 1}^2}{1/\sigma_{\epsilon 1}^2 + 1/\sigma_{\epsilon 2}^2 + 1/\sigma_{\epsilon 3}^2} \\ \frac{1/\sigma_{\epsilon 2}^2}{1/\sigma_{\epsilon 1}^2 + 1/\sigma_{\epsilon 2}^2 + 1/\sigma_{\epsilon 3}^2} \\ \frac{1/\sigma_{\epsilon 3}^2}{1/\sigma_{\epsilon 1}^2 + 1/\sigma_{\epsilon 2}^2 + 1/\sigma_{\epsilon 3}^2} \end{pmatrix} \quad (4)$$

When only two datasets are considered for fusion as per the decision map, the weights are computed as,

$$\begin{pmatrix} w_1 \\ w_2 \end{pmatrix} = \begin{pmatrix} \frac{1/\sigma_{\epsilon 1}^2}{1/\sigma_{\epsilon 1}^2 + 1/\sigma_{\epsilon 2}^2} \\ \frac{1/\sigma_{\epsilon 2}^2}{1/\sigma_{\epsilon 1}^2 + 1/\sigma_{\epsilon 2}^2} \end{pmatrix}, \begin{pmatrix} w_2 \\ w_3 \end{pmatrix} = \begin{pmatrix} \frac{1/\sigma_{\epsilon 2}^2}{1/\sigma_{\epsilon 2}^2 + 1/\sigma_{\epsilon 3}^2} \\ \frac{1/\sigma_{\epsilon 3}^2}{1/\sigma_{\epsilon 2}^2 + 1/\sigma_{\epsilon 3}^2} \end{pmatrix}, \begin{pmatrix} w_1 \\ w_3 \end{pmatrix} = \begin{pmatrix} \frac{1/\sigma_{\epsilon 1}^2}{1/\sigma_{\epsilon 1}^2 + 1/\sigma_{\epsilon 3}^2} \\ \frac{1/\sigma_{\epsilon 3}^2}{1/\sigma_{\epsilon 1}^2 + 1/\sigma_{\epsilon 3}^2} \end{pmatrix} \quad (5)$$

When only one of three surface soil moisture datasets is available, that dataset will be used right away during the fusion process with weightage of unity and zero weightage to the others.

Finally, fused soil moisture value at a pixel is calculated as,

$$SM_{fused} = (w_1 \times SM_1) + (w_2 \times SM_2) + (w_3 \times SM_3) \quad (6)$$

where (w_1, w_2, w_3) signifies the weightage value assigned to each of the three-satellite dataset and (SM_1, SM_2, SM_3) depicts the corresponding satellite soil moisture values for the pixel.

4. Results and discussion

4.1. Quantification of bias in satellite soil moisture data

Error structure in the soil moisture data is quantified spatially over India by calculating the error variance (σ_ϵ^2) and correlation coefficient (ρ^2) using ETC analysis. Spatial variation of the 90th percentile of error variance (σ_ϵ^2) and correlation coefficient (ρ^2), for SMAP, AMSR-2, and SMOS, are depicted in Figure 3.

SMAP exhibits least error variance in the range 0–0.002, covering around 65.9% of India. While, for the same error variance range, the coverage of AMSR-2 is limited to only 29%, followed by SMOS with the least spatial coverage of 19%. Lower error variance metric implies less variability of satellite retrieved data with respect to ground truth, suggesting higher accuracy and reliability. To provide a more comprehensive evaluation, correlation coefficients were also analysed to assess the agreement between satellite-derived and ground truth data. It reflects the ability of satellite data to track ground truth variations, offering insights into the overall accuracy and consistency of the dataset. For the range of 0.8–1, SMAP has 38%, which reduced to 22.6% for AMSR-2 and 15% for SMOS,

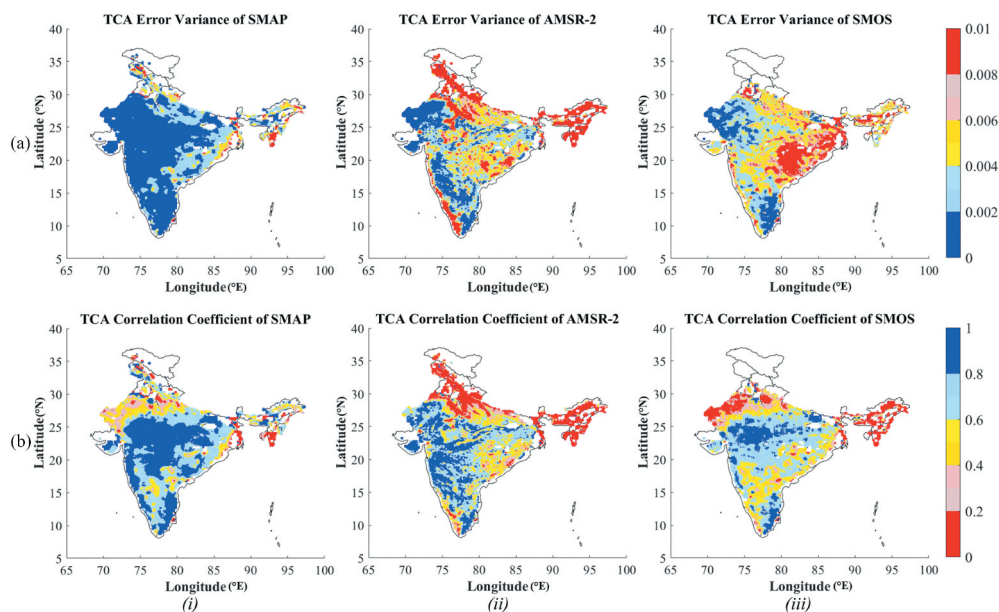


Figure 3. Spatial distribution of (a) error variance and (b) correlation coefficient for three datasets – SMAP, AMSR-2, and SMOS.

underscoring the superior performance of SMAP in terms of providing accurate soil moisture data.

A comprehensive analysis of error structure of individual dataset showed that SMAP has minimum variability of error variance values with median lying at 0.0014, followed by AMSR-2 at 0.0032 and SMOS with the highest median at 0.0038 (Figure 4). This signifies the lowest variability of the SMAP dataset with respect to actual ground data. In terms of correlation coefficient values, SMAP showed the highest correlation coefficient values with median lying at 0.746, followed by AMSR-2 and SMOS at 0.639 and 0.615 respectively. The pattern suggests that SMAP not only offers lower error variances but also maintains higher reliability in capturing soil moisture dynamics when compared to AMSR-2 and SMOS.

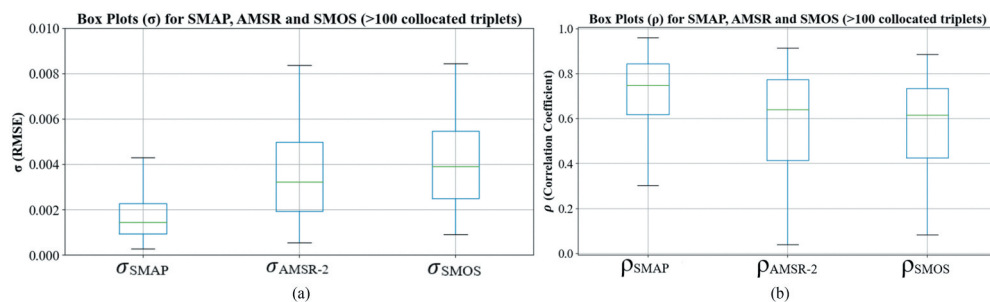


Figure 4. Dispersion of (a) error variance and (b) correlation coefficient (right) for datasets (SMAP, AMSR-2, SMOS) respectively, shown as boxplots.

Notably, it was hypothesized that SMAP, operating in L-band (~1.41 GHz) and featuring Radio Frequency Interference (RFI) mitigation techniques, would outperform other products over India (Chakravorty et al. 2016). However, a comparative analysis (Figure 5) revealed that while SMAP generally exhibited low error variances, it showed limitations in accurately capturing soil moisture in BWh (hot desert) and BSh (hot semi-arid) climatic zones, particularly in western and south-western regions of India. This was evident by SMAP's reduced correlation coefficients in these areas, suggesting a weaker relationship with ground data. Conversely, AMSR-2 demonstrated superior performance in these climatic zones, with lower error variances and consistently higher correlation coefficients, thus effectively capturing soil moisture dynamics. AMSR-2's robust performance in arid regions may be attributed to its sensor's resilience to sunlight, clouds, and dust alongside its efficiency in analysing surface moisture in sparsely vegetated areas (Wu et al. 2016; Gade et al., 2023; Rao & Chaudhari, 2009). This efficacy is further supported by its extensive spatial and temporal data coverage, which provides a more reliable sample for error analysis (Hu et al. 2022).

This analysis underscores AMSR-2's adaptability to BWh and BSh zones, suggesting that soil moisture retrieval algorithms for SMAP require re-evaluation to improve accuracy in these areas. Ma et al. (2019) also highlighted the need for further improvement in the L-band (SMAP, SMOS) products in tropical or desert regions. Therefore, AMSR-2's observations may be preferentially weighted in these climatic zones to enhance the fused product's reliability and accuracy.

The seasonal dynamics of error variance are examined, as shown in Figure 6. The spatial plots of temporal variation of error are shown in the supplementary material (Figure S1). This analysis explores how error variance fluctuates over the seasons as categorized by IMD: Winter (January-February), Pre-monsoon (March-April-May), Monsoon (June-July-August-September) and Post-monsoon (October-November-December). A consistent increase in error variance was observed across all three products (SMAP, AMSR-2, SMOS) during the onset of monsoon, with SMAP exhibiting the smallest increase. The increase in error variance can be attributed to dynamic changes in vegetation cover, including dense vegetation growth during the monsoon which can attenuate microwave signals differently, leading to uncertainties in soil moisture retrievals. During the pre-monsoon season, an increase in error variance was noted, potentially influenced by extensive irrigation

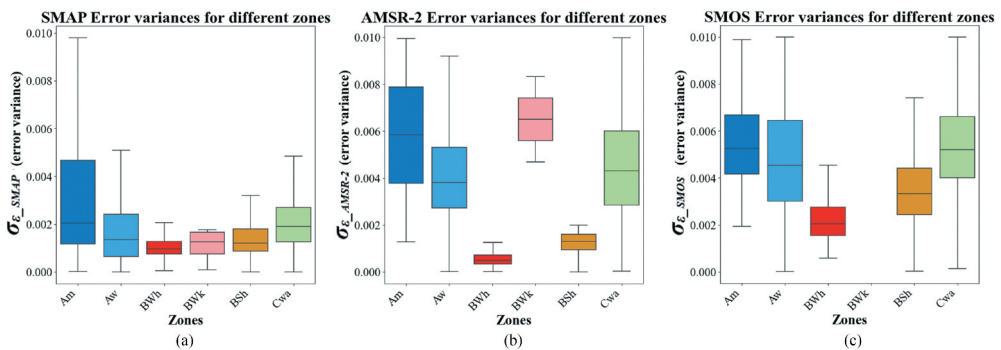


Figure 5. Spatial variation of error structure of (a) SMAP, (b) AMSR-2, (c) SMOS over six major climatic zones of India (Am, Aw, BWh, BWk, BSh, Cwa).

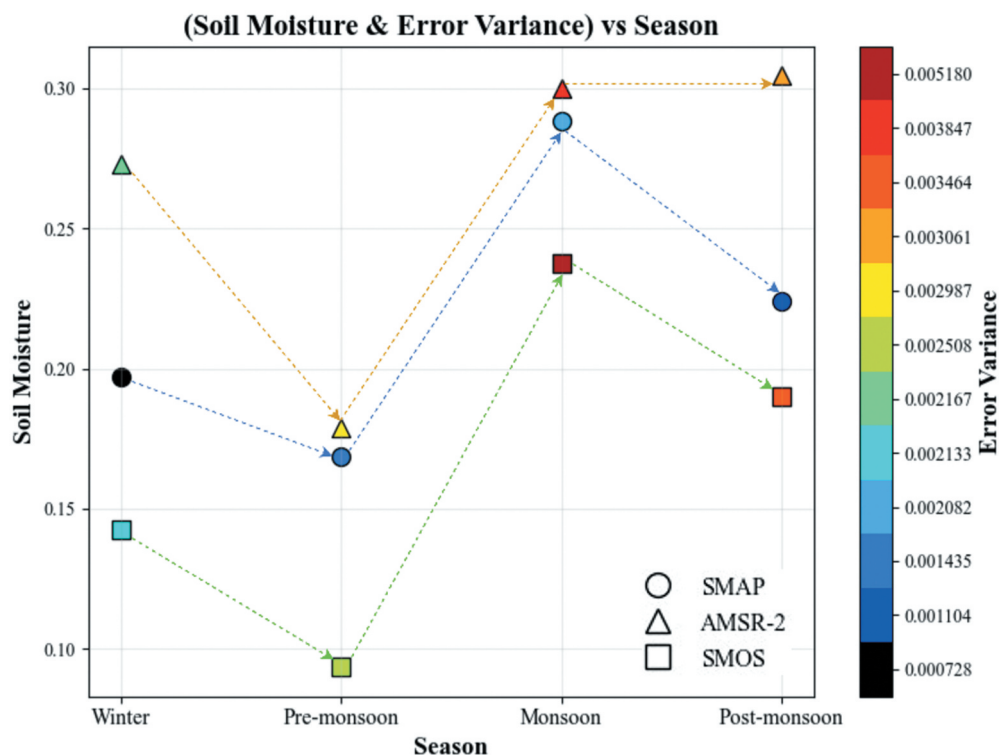


Figure 6. Seasonal variation between soil moisture and error variance.

activities for agriculture, causing more attenuation and dispersion of microwave signals. Moreover, the inherent coarser resolution of original SMOS and AMSR-2 products contributes to discrepancies in capturing small-scale soil moisture variability, particularly problematic in areas with diverse land cover, where finer spatial resolution is crucial for accurate soil moisture detection, leading to increased error variance in these products. It is deduced from this comprehensive analysis that data fusion strategy should be applied consistently throughout the year rather than limiting to specific time period of the year, to accommodate the temporal variability observed across different seasons.

4.2. Influence of rainfall and irrigation

Satellite-retrieved data captures the surface soil moisture layer up to few centimetres i.e. $\sim (3\text{--}5)$ cm, the layer that quickly responds to precipitation events, outcomes of which are distinctly reflected in the soil moisture datasets. This study quantitatively assessed the correlation between soil moisture and precipitation across India's diverse climatic zones. SMAP consistently demonstrated highest correlation coefficients, indicating its superior capability to accurately capture precipitation events when compared to AMSR-2 and SMOS data. For this purpose, we used standard Level-3 daily soil moisture products, which provide daily composites rather than separate AM and PM overpass retrievals. Therefore, the results are based on daily aggregated values rather than specific overpass time. The overpass timing can influence soil moisture-precipitation relationships,

particularly in regions such as India where afternoon precipitation events and irrigation activities introduce strong diurnal variability. Because daily aggregated products were used, these diurnal effects are partially smoothed in our analysis. Importantly, all datasets were evaluated under the same daily temporal framework, ensuring that the relative performance comparison and fusion outcomes remain valid. MI analysis was subsequently performed based on these correlations, providing a robust framework for assessing the complementary information content of the different datasets. Future studies could explore explicit AM versus PM retrievals to better capture diurnal soil moisture dynamics.

Further, the seasonality of soil moisture and precipitation data when averaged spatially across India (Figure 7(a)) reinforced the robust performance of SMAP, with highest correlation of 0.93 with IMD precipitation dataset, higher than SMOS at 0.84 and AMSR-2 at 0.65. This comprehensive evaluation, incorporating ETC and considering spatial, temporal, and meteorological aspects, conclusively shows that the SMAP outperforms AMSR-2 and SMOS across most regions of India.

While SMAP demonstrated the highest correlation with precipitation indicating robust tracking of precipitation-induced soil moisture variations, it is important to note that not all the soil moisture variations can be attributed to rainfall, and there may exist high soil moisture values even in the absence of precipitation events, showcasing weaker relationship between them (Figure 7(b)). As in most of the agricultural regions in North India, irrigation practices are adopted to meet the water demand of the crops throughout various stages of growth. Irrigation factor, independent of rainfall, significantly alters the soil moisture profiles. Therefore, we investigated the ability of SMAP soil moisture product to capture irrigation events. Rainfall ≥ 0.5 mm/day and <0.5 mm/day are used to consider a rainy and non-rainy event respectively, as very light precipitation is statistically unreliable for both the rain gauge stations and satellite precipitation measurements (Chaudhary and Dhanya 2020; Sunilkumar et al. 2015; Tang et al. 2015). As soil moisture value fluctuates between 0 and 1, implying very dry and saturation conditions respectively, a range of 0.25 to 0.55 is considered as an optimum soil moisture value for plant growth as it covers most of the soil types (including sandy, loamy, silty, clay and their different combinations) under various climatic conditions across India (following the conclusions derived by Archontoulis et al. (2020) and Dietzel et al. (2016)). Further, we

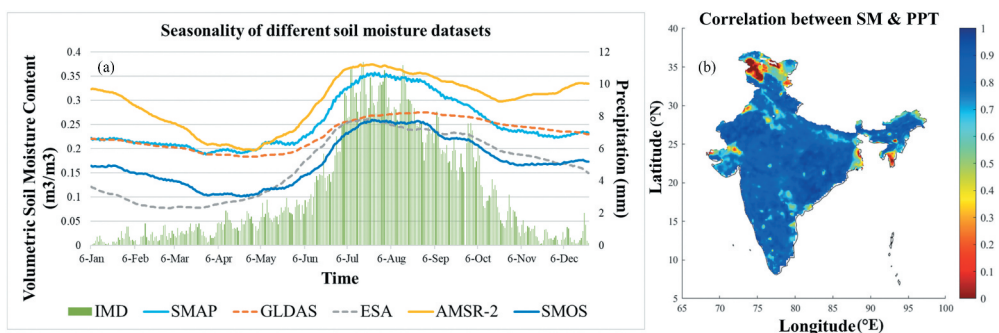


Figure 7. (a) Seasonality of (SMAP, AMSR-2, SMOS) soil moisture and IMD precipitation data, spatially averaged over whole India, (b) correlation of SMAP soil moisture with IMD precipitation data.

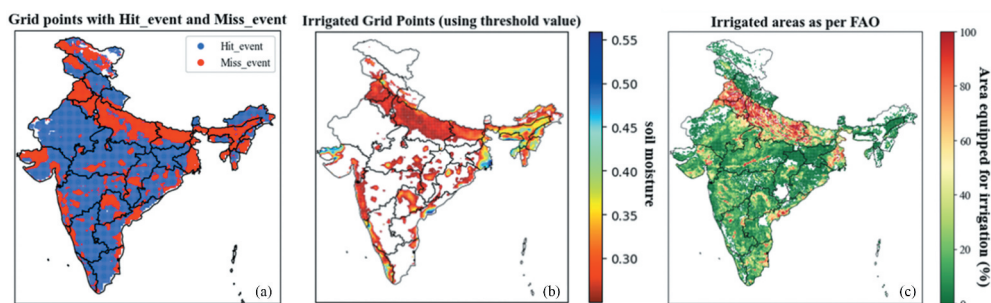


Figure 8. (a) grid points corresponding to hit and miss events, (b) potential irrigated grid points (using SMAP), (c) percentage of area equipped for irrigation.

hypothesize that when precipitation is <0.5 mm/day but soil moisture value is >0.25 m³/m³; it reflects a miss event, highlighting the potential irrigated regions where existing soil moisture values are high in the absence of rainy events, otherwise it reflects a hit event where precipitation is >0.5 mm/day and soil moisture value is >0.25 m³/m³. The spatial variation of hit and miss events is shown in Figure 8(a). It was noticed that most of the resulting grid points of miss events are lying in Indo-Gangetic plain (Figure 8(b)) which is proved to be the largely irrigated area over India region.

Upon comparing the results with FAO irrigation data of the parameter 'percentage of area equipped for irrigation' (shown in Figure 8(c)), it was observed that the percentage of area equipped for irrigation lying between 60% and 100%, predominantly covering the Indo-Gangetic plains, is accurately represented by SMAP data. The temporal analysis further revealed that these irrigation signatures prominently emerge during the rabi crops season (October-December), a period characterized by minimal rainfall in India. Consequently, irrigation practices predominantly meet the crop water requirement during this season. While SMAP dataset effectively captures irrigation patterns, particularly in Indo-Gangetic plains, it also indicates other parts of eastern and south-western regions of India as irrigated areas. It can be attributed to the higher rainfall in the regions, which naturally maintains high soil moisture values, thus challenging the threshold condition used for detecting irrigation signals. Hence, a deeper investigation into differentiating irrigation-induced and rainfall-induced soil moisture variations, while considering diverse soil types, crop types, and climatic conditions across India, is required to optimize soil moisture assessments for improved agricultural and hydrological modelling.

4.3. Assessing satellite soil moisture and precipitation dependency

In the absence of a dense network of in-situ ground stations in India, this study considered large-scale precipitation data as a proxy to validate satellite-derived soil moisture products. By analysing the joint and marginal probability distributions, MI values are calculated to quantify the non-linear relationship between soil moisture and precipitation. Higher MI values indicate a strong alignment of satellite soil moisture data with observed precipitation patterns, that further indicate an effective validation of the product. This

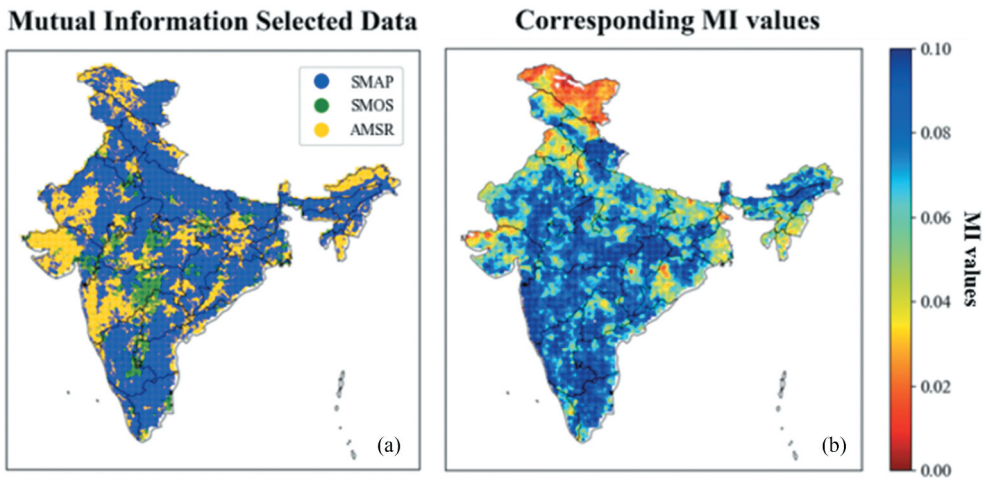


Figure 9. (a) choice map from MI analysis indicating which data is best at a certain grid point i.e. SMAP (blue), AMSR-2 (yellow), SMOS (green). (b) MI value corresponding to selected dataset.

method provides a critical assessment tool in regions where conventional ground-based validation is limited.

After calculating MI values between each of SMAP, AMSR-2, and SMOS product with respect to IMD precipitation data, a choice map based on MI analysis is plotted. Figure 9(a) illustrates the grids where SMAP/SMOS/AMSR displayed the highest MI value. SMAP covered around 60% area with highest MI value, followed by AMSR-2 in 30%, and SMOS in 10%. The corresponding high MI values at each grid are shown in Figure 9(b).

Notably, AMSR-2 again showed high MI values in the western and south-western Indian regions (Figure 9(a)), which re-confirmed its superior performance from ETC analysis, i.e. in BWh and BSh climatic zones (detailed comparison is shown in Figure S2). A potential reason for AMSR-2 soil moisture product's enhanced performance in these areas could be its frequent observations cycle with more spatial coverage under 2 days temporal resolution in comparison to SMAP and SMOS, which enables more effective monitoring of soil moisture fluctuations in regions characterized by limited rainfall and high evaporation rates.

4.4. Generation of final fused product

The best grid points for each satellite product SMAP, AMSR-2, and SMOS were identified based on ETC analysis, i.e. grid points with lowest error variance and highest correlation coefficient values. A comparative analysis between the best grid points of AMSR-2 product from ETC and those from MI analysis revealed a remarkable consistency in AMSR-2's performance across both the methodologies. This consistent performance suggests that though SMAP is better for the majority of the grids, AMSR-2 should be preferentially included for regions where it showed superior performance (highlighted in Figure S2). Such integration could leverage the strengths of AMSR-2 in capturing soil moisture dynamics under these specific climatic conditions. The comprehensive analysis of all the grid points across Indian region at a spatial resolution of 9 km further elaborates

diverse scenarios emerging from both ETC and MI analysis. Through MI, the best-performing grid points were identified for SMAP, AMSR-2, and SMOS individually, highlighting the specific regions where each product excels. ETC further extended this evaluation by incorporating the combined performance of multiple products. This analysis revealed regions where SMAP, AMSR-2, or SMOS performed optimally as single products, as well as areas where combinations of two or more products, such as (SMAP & AMSR-2), (AMSR-2 & SMOS), or (SMAP & SMOS), achieved superior accuracy. Notably, certain grid points demonstrated the highest reliability when all three products (SMAP, AMSR-2, & SMOS) were utilized together. Following these findings, a decision map was created (Figure 10) showing the relative efficacy of individual and combined products, as it illustrates the distribution of best soil moisture products over India. The decision map improves soil moisture retrieval accuracy and reliability by identifying places where either specific or a combination of products perform the best.

Contrary to typical approaches in the existing literature, which often apply a uniform fusion algorithm across the entire study area without considering the strengths and weakness of the individual datasets, we questioned the necessity of fusion at each specific grid point, and suggested fusion only where it adds value, thereby enhancing the precision and applicability of the final fused soil moisture dataset. The decision map

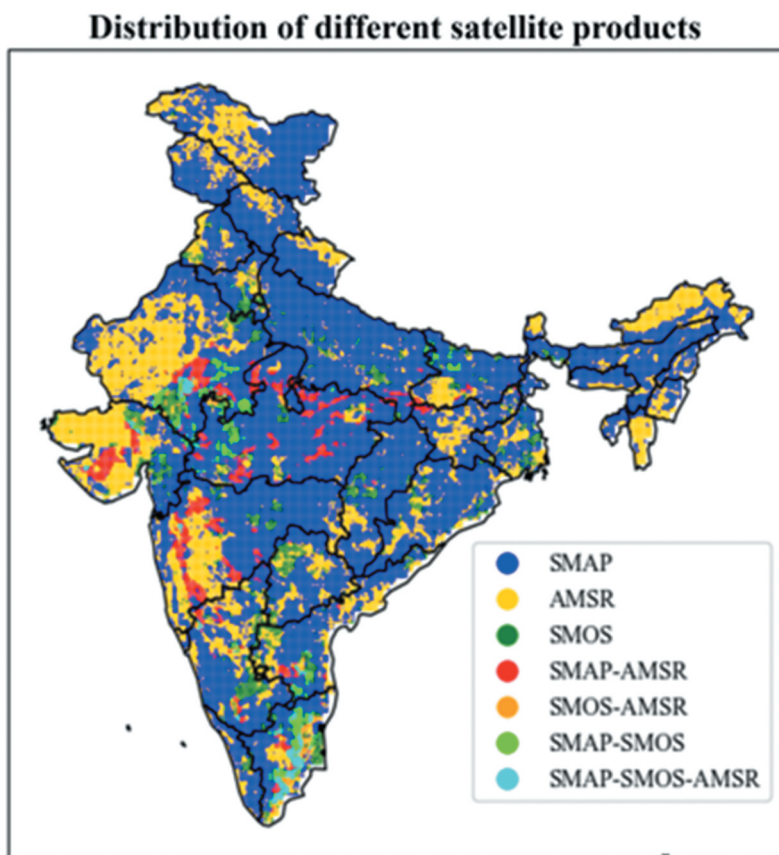


Figure 10. Final decision map showing distribution of satellite products (SMAP, AMSR-2, SMOS).

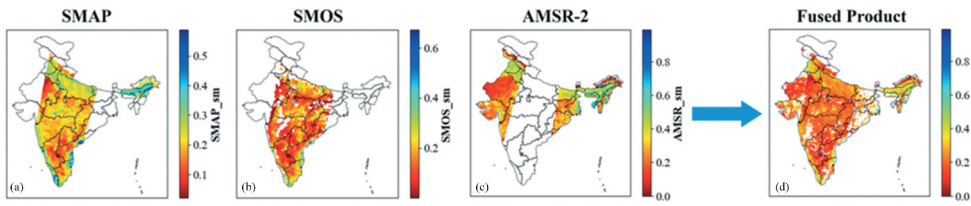


Figure 11. LWF applied to dataset (a) SMAP, (b) SMOS, (c) AMSR-2 in order to produce (d) fused product.

excludes those grid points where a single dataset (either SMAP, AMSR-2, or SMOS) is the best from the fusion process, i.e. linear weight fusion algorithm will retain the original dataset for those locations. Conversely, at grid points where the decision map identifies a combination of two or all three datasets (SMAP, AMSR-2, SMOS), the fusion algorithm engages Equation 4 or 5, respectively. These equations integrate the error variance derived from the ETC analysis to calculate and assign appropriate weightages to each dataset. Subsequently, Equation 6 is applied to fuse the datasets, to generate a comprehensive soil moisture value for each grid point as indicated by the decision map. This method ensures that the fusion process is dynamically adjusted to enhance soil moisture estimation accuracy based on the specific data characteristics and error metrics of each grid point.

The LWF algorithm integrates the three soil moisture products from 2016 to 2019, resulting in a synthesized soil moisture dataset, as presented in Figure 11. The final fused product is expected to exhibit enhanced potential for assimilation into hydrological models, especially for applications in drought monitoring.

4.5. Performance analyses of fused product

Initially, ETC analysis is reapplied to evaluate and compare the error characteristics of the fused product against those of the original individual datasets. This step ensures that any improvements in error metrics due to the fusion process are quantitatively assessed. Subsequently, the fused product is assessed against the modelled/reanalysis soil moisture datasets, i.e. GLEAM and ERA5. Correlations are calculated and spatially plotted for the relationships between the fused product and GLEAM, as well as fused product and ERA5. Given that the decision map indicates SMAP as the optimal product across more than 85% of the spatial domain, these correlation plots are then compared with those of SMAP against GLEAM and ERA5. The analysis highlighted areas where the fused product outperforms SMAP, with the observed differences being consistent across both GLEAM and ERA5, particularly in regions where the decision map does not identify SMAP as the best product. Finally, the accuracy of the fused product is validated by comparison with in-situ soil moisture data from three stations: Singanallur (SGR), Madahalli (MDH), and Berambadi (BMB), which are included in the Indian COSMOS Network (ICON). This comprehensive validation approach provides a robust assessment of the fused product's performance, ensuring its reliability for practical applications in hydrological modelling and monitoring.

4.5.1. Performing ETC on fused soil moisture product

ETC analysis was conducted with the fused product included with the triplet configuration [FUSED PRODUCT – GLDAS – ESA_ACTIVE], replacing the passive products that included (SMAP, AMSR-2, SMOS). This process of reapplication of ETC on the fused product was carried out as a diagnostic and consistency analysis to examine the relative error characteristics of the fused product under same reference framework used for the input datasets. It is important to note that this analysis does not represent an independent validation of the fused soil moisture product, and the primary and independent evaluation of the fused product is based on in-situ soil moisture measurements (Section 4.5.3.). The ETC results presented here are intended to provide insights into changes in error and correlation structure following the fusion process. The spatial plots of ETC analysis, as shown in Figure 12, indicate that the fused product generally exhibits lower random error variance and higher correlation coefficients relative to individual passive products, particularly in regions where SMAP previously underperformed, such as BWh and BSh climatic zones of western and south-western India. This improvement highlights the efficacy of integrating AMSR-2 characteristics, which are particularly robust in arid zones, into the fused product. Overall, this analysis suggests that the decision map-based fusion framework effectively adapts to regional differences in product performance and improve the internal consistency of soil moisture estimates across diverse hydro-climatic regimes in India.

4.5.2. Comparison with GLEAM and ERA5 soil moisture products

The fused soil moisture product is evaluated against the GLEAM (Miralles et al., 2010; Martens et al., 2017) and ERA5 (W. Dorigo et al. 2017) datasets. Given that the decision map indicates SMAP as the optimal product across more than 85% of the spatial domain, the fused product is specifically assessed in regions where SMAP is not identified as the superior product. Accordingly, comparisons are conducted between the fused soil moisture product and SMAP.

Spatial correlation analysis is performed between the fused product with GLEAM and ERA5, as well as for SMAP with GLEAM and ERA5. Given the observed similarity

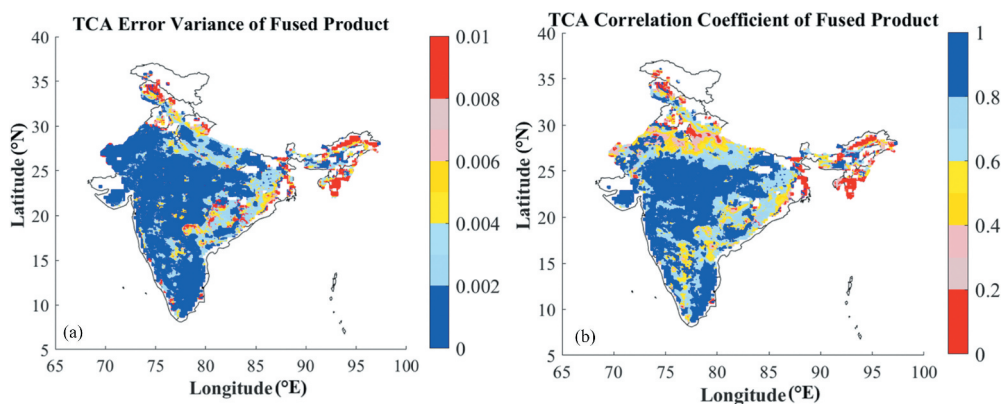


Figure 12. (a) error variance and (b) correlation coefficient of fused soil moisture product.

in the spatial correlation patterns, the correlation differences between the fused and SMAP soil moisture products are plotted, using both GLEAM and ERA5 as reference datasets, as illustrated in Figure 13. Regions where the fused soil moisture product exhibits a higher correlation with GLEAM or ERA5 compared to SMAP are indicated in blue. Conversely, red regions denote areas where SMAP shows a stronger correlation with GLEAM or ERA5 than the fused product. With respect to the decision map, it is evident that the majority of blue regions align with areas where SMAP is not identified as the best product, with other products, such as AMSR-2 or their combinations, prevailing. These findings suggest that the fused product demonstrates a stronger correlation, i.e. its soil moisture estimates are more closely aligned with the GLEAM or ERA5 values than those of the SMAP product. Thus, the fused product offers enhanced accuracy over individual products, particularly SMAP, when benchmarked against modelled or reanalysis datasets.

4.5.3. Comparison with in-situ ground data

The evaluation of the fused soil moisture product against individual datasets was rigorously conducted to determine if it exhibits superior error characteristics, i.e. specifically lower error variance and higher correlation coefficient. In-situ soil moisture data from three COSMOS network stations SGR, MDH, and BMB, which monitors the top 5 cm of the surface soil moisture layer, were utilized in this analysis. Since COSMOS was launched in 2015 in India, the availability of in-situ data from 2016 to 2019 aligns with our study period, enabling a direct comparison of the datasets. Figure 14 validates the efficacy of the decision map, i.e. it shows that the fusion algorithm optimally selected SMAP as predominant product over the grid points where these stations are located. This selection is evident from the scatter plots in Figure 14, where the fused soil moisture product and SMAP data exhibit similar patterns, confirming the reduced variability and high correlation coefficients at 0.78, 0.83 and 0.69 for SGR, MDH and BMB, respectively. Figure 14 shows the

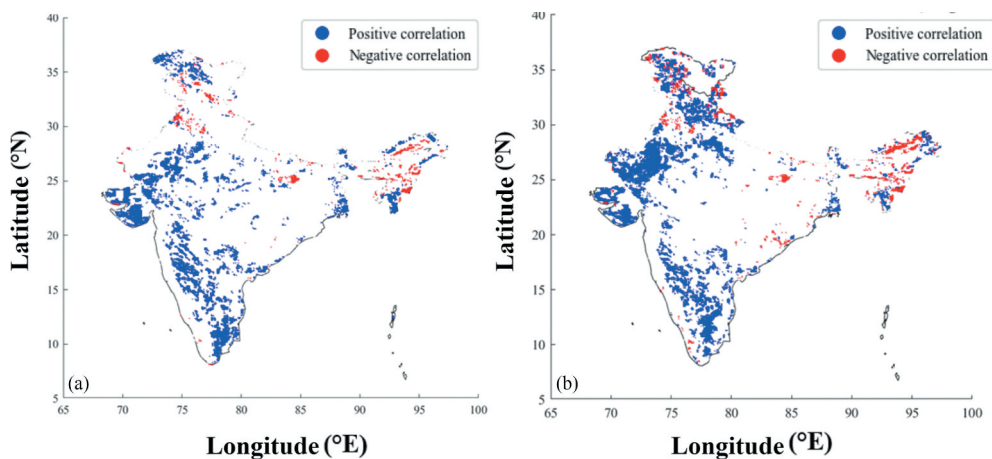


Figure 13. Correlation difference between fused and SMAP soil moisture product, using (a) GLEAM, (b) ERA5.

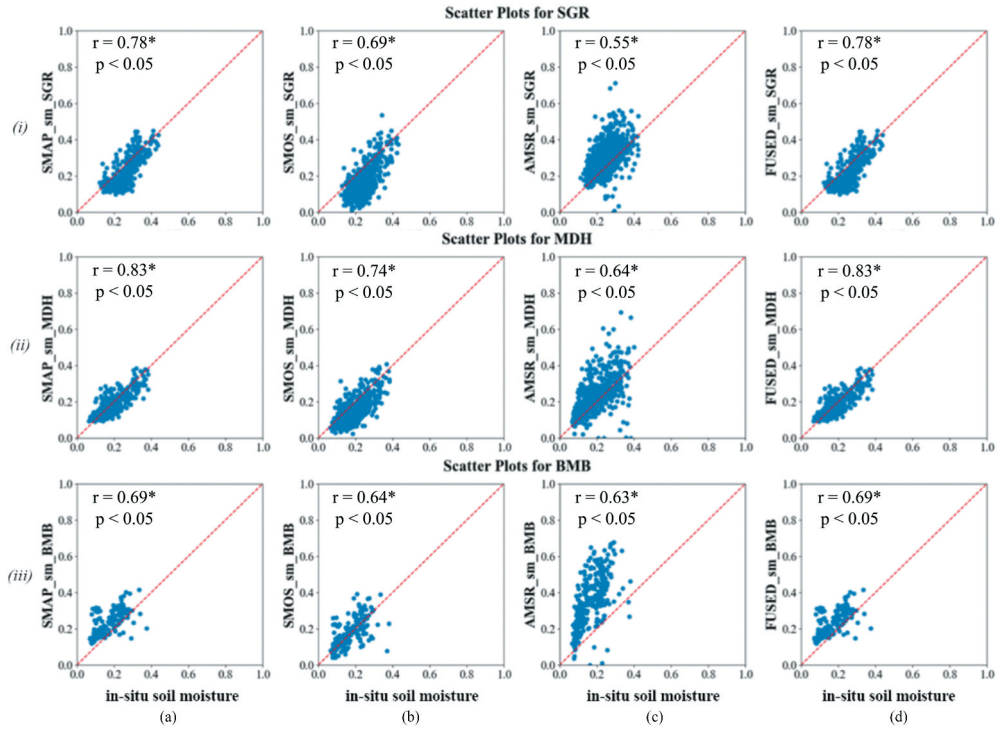


Figure 14. Scatter plots for (a) SMAP, (b) SMOS, (c) AMSR-2 and (d) fused soil moisture products at (i) Singanallur, (ii) Madahalli, and (iii) Berambadi; where correlations (r) are considered statistically significant at a significance level of 0.05.

corresponding correlations (r) and their statistical significance ($p < 0.05$) for each subplot. The time series plots for visualizing the temporal dynamics and assessing the performance of fused soil moisture product over time are shown in Figure S3. While the identical behaviour of the fused product with SMAP in scatter plot indicates limited addition value of fusion at these particular locations, the broader advantage of the method lies in enhancing spatial coverage and temporal completeness. As shown in Figure 11(d), the fused dataset consistently provides more spatial coverage than any single product alone, thereby improving data availability over the entire study domain and period.

This alignment demonstrates the fused product's reliability and its enhanced performance in capturing accurate soil moisture levels compared to the individual products. AMSR-2 soil moisture product tends to overestimate soil moisture values, with correlation coefficient value of 0.55, 0.64 and 0.63 at SGR, MDH and BMB stations respectively. Conversely, the SMOS product generally underestimates soil moisture values, achieving correlation coefficients of 0.69, 0.74 and 0.64 at these same stations. This variation in performance highlights the distinct characteristics and potential biases inherent in each satellite product.

5. Conclusions

Soil moisture being a crucial variable affects land-atmosphere interactions, plant development, and water availability in the hydrological cycle. And hence, understanding its variability is pivotal in studying and managing hydrological and climatic extremes. This study utilized ETC and MI analysis to enhance the accuracy of satellite-derived soil moisture estimates across India, a region with limited in-situ ground soil moisture data network and high reliance on remote sensing-based data. The findings claim that the LWF technique, informed by ETC and MI analysis, successfully integrated the strengths of SMAP, AMSR-2 and SMOS, creating a superior soil moisture dataset. Notably, SMAP displayed the lowest error variances and highest correlation coefficients overall, underscoring its efficacy in most of India except for BWh and BSh zones where AMSR-2 outperformed, suggesting the need for product-specific applications based on regional climatic conditions.

The new soil moisture data from this selective fusion approach demonstrated significant improvements in soil moisture accuracy, particularly in hot desert and semi-arid regions. Validation against modelled/reanalysis products like GLEAM and ERA5, and in-situ data from COSMOS network confirmed the fused product's enhanced performance. This fused dataset not only reduces dependence on any single satellite product but also offers broader spatial and temporal coverage, improving the detection and characterization of extreme hydrological events. In extreme weather conditions, the fused product delivers robust estimates from several sources, reducing the risks of dependency on a single remote sensing product and minimizing potential misinterpretations or overlooked events.

This research has laid a foundation for integrating soil moisture data into hydrological models more effectively, enhancing their ability to forecast and manage climatic extremes like floods and droughts. The advanced analytical methodologies employed here offer robust framework for future enhancements in remote sensing applications, providing a pathway towards more resilient and accurate environmental management and disaster mitigation strategies. These conclusions underscore the importance of selective satellite data fusion techniques to address specific regional challenges, advancing our capability to manage water resources and predict natural disasters in a changing climate. This soil moisture data has crucial practical applications in the development of early-warning drought monitoring systems, where agricultural and ecological stakes are high, including other applications in water resource management, and climate science, highlighting the importance of accurate soil moisture data in sustainable environmental management.

Disclosure statement

No potential conflict of interest was reported by the author(s).

Data availability statement

Data will be made available from the authors, upon reasonable request.

References

- Ajaz, A., and S. Taghvaeian. 2018. Tracking Drought Using Soil Moisture Information.
- Al Bitar, A., A. Mialon, Y. H. Kerr, F. Cabot, P. Richaume, E. Jacqueline, A. Quesney, et al. 2017. "The Global SMOS Level 3 Daily Soil Moisture and Brightness Temperature Maps." *Earth System Science Data* 9 (1): 293–315. <https://doi.org/10.5194/essd-9-293-2017>.
- Archontoulis, S. V., M. J. Castellano, M. A. Licht, V. Nichols, M. Baum, I. Huber, R. Martinez-Feria, et al. 2020. "Predicting Crop Yields and Soil-Plant Nitrogen Dynamics in the US Corn Belt." *Crop Science* 60 (2): 721–738. <https://doi.org/10.1002/csc2.20039>.
- Beck, H. E., N. E. Zimmermann, T. R. McVicar, N. Vergopolan, A. Berg, and E. F. Wood. 2018. "Present and Future Köppen-Geiger Climate Classification Maps at 1-Km Resolution." *Scientific Data* 5 (1): 180214. <https://doi.org/10.1038/sdata.2018.214>.
- Bharti, V., C. Singh, J. Ettema, and T. A. R. Turkington. 2016. "Spatiotemporal Characteristics of Extreme Rainfall Events Over the Northwest Himalaya Using Satellite Data." *International Journal of Climatology* 36 (12): 3949–3962. <https://doi.org/10.1002/joc.4605>.
- Chakravorty, A., B. R. Chahar, O. P. Sharma, and C. T. Dhanya. 2016. "A Regional Scale Performance Evaluation of SMOS and ESA-CCI Soil Moisture Products Over India with Simulated Soil Moisture from MERRA-Land." *Remote Sensing of Environment* 186:514–527. <https://doi.org/10.1016/j.rse.2016.09.011>.
- Chaudhary, S., and C. T. Dhanya. 2020. "Expanding Contingency Table for Intensity and Frequency Based "True" Detection of Rainy Events in Precipitation Datasets." *Atmospheric Research* 244:105119. <https://doi.org/10.1016/j.atmosres.2020.105119>.
- Cheema, M. J. M., W. G. M. Bastiaanssen, and M. M. Rutten. 2011. "Validation of Surface Soil Moisture from AMSR-E Using Auxiliary Spatial Data in the Transboundary Indus Basin." *Journal of Hydrology* 405 (1–2): 137–149. <https://doi.org/10.1016/j.jhydrol.2011.05.016>.
- Das, N. N., Entekhabi D., Kim, S., Yueh, S., and O'Neill, P. 2016, July. "Combining SMAP and Sentinel data for high-resolution Soil Moisture product." In *2016 IEEE International Geoscience and Remote Sensing Symposium (IGARSS)* 129–131.
- Dietzel, R., M. Liebman, R. Ewing, M. Helmers, R. Horton, M. Jarchow, and S. Archontoulis. 2016. "How Efficiently Do Corn- and Soybean-Based Cropping Systems Use Water? A Systems Modeling Analysis." *Global Change Biology* 22 (2): 666–681. <https://doi.org/10.1111/gcb.13101>.
- Dingman, S. L. (2015). *Physical hydrology*. Waveland press.
- Dorigo, W. A., K. Scipal, R. M. Parinussa, Y. Y. Liu, W. Wagner, R. A. M. de Jeu, and V. Naeimi. 2010. "Error Characterisation of Global Active and Passive Microwave Soil Moisture Datasets." *Hydrology and Earth System Sciences* 14 (12): 2605–2616. <https://doi.org/10.5194/hess-14-2605-2010>.
- Dorigo, W. A., W. Wagner, R. Hohensinn, S. Hahn, C. Paulik, A. Xaver, A. Gruber, et al. 2011. "The International Soil Moisture Network: A Data Hosting Facility for Global in situ Soil Moisture Measurements." *Hydrology and Earth System Sciences* 15 (5): 1675–1698. <https://doi.org/10.5194/hess-15-1675-2011>.
- Dorigo, W. A., A. Xaver, M. Vreugdenhil, A. Gruber, A. Hegyiová, A. D. Sanchis-Dufau, D. Zamojski, C. Cordes, W. Wagner, and M. Drusch. 2013. "Global Automated Quality Control of in Situ Soil Moisture Data from the International Soil Moisture Network." *Vadose Zone Journal* 12 (3): 1–21. <https://doi.org/10.2136/vzj2012.0097>.
- Dorigo, W., W. Wagner, C. Albergel, F. Albrecht, G. Balsamo, L. Brocca, D. Chung, et al. 2017. "ESA CCI Soil Moisture for Improved Earth System Understanding: State-of-the-Art and Future Directions." *Remote Sensing of Environment* 203:185–215. <https://doi.org/10.1016/j.rse.2017.07.001>.
- Draper, C., R. Reichle, R. de Jeu, V. Naeimi, R. Parinussa, and W. Wagner. 2013. "Estimating Root Mean Square Errors in Remotely Sensed Soil Moisture Over Continental Scale Domains." *Remote Sensing of Environment* 137:288–298. <https://doi.org/10.1016/j.rse.2013.06.013>.
- Engman, E. T., and N. Chauhan. 1995. "Status of Microwave Soil Moisture Measurements with Remote Sensing." *Remote Sensing of Environment* 51 (1): 189–198. [https://doi.org/10.1016/0034-4257\(94\)00074-W](https://doi.org/10.1016/0034-4257(94)00074-W).
- Entekhabi, D. 1995. "Recent Advances in Land-Atmosphere Interaction Research." *Reviews of Geophysics* 33 (S2): 995–1003. <https://doi.org/10.1029/95RG01163>.

- Entekhabi, D., E. G. Njoku, P. E. O'Neill, K. H. Kellogg, W. T. Crow, W. N. Edelstein, J. K. Entin, et al. 2010. "The Soil Moisture Active Passive (SMAP) Mission." *Proceedings of the IEEE* 98 (5), Article 704–716. <https://doi.org/10.1109/JPROC.2010.2043918>.
- Erdenebat, E., and T. Sato. 2018. "Role of Soil Moisture-Atmosphere Feedback During High Temperature Events in 2002 Over Northeast Eurasia." *Progress in Earth and Planetary Science* 5 (1): 37. <https://doi.org/10.1186/s40645-018-0195-4>.
- Gade, S. A., J. V. Yadav, S. P. Shinde, D. D. More, K. R. Gadekar, and V. Nikam. 2023. "Variability in Soil Moisture Using AMSR-E Product- a Regional Case Study in the Province of Marathwada Division, India." *Geology, Ecology, and Landscapes* 7 (2): 115–125. [10.1080/24749508.2021.1943811](https://doi.org/10.1080/24749508.2021.1943811).
- Gruber, A., W. A. Dorigo, W. Crow, and W. Wagner. 2017. "Triple Collocation-Based Merging of Satellite Soil Moisture Retrievals." *IEEE Transactions on Geoscience & Remote Sensing* 55 (12): 6780–6792. <https://doi.org/10.1109/TGRS.2017.2734070>.
- Gruber, A., T. Scanlon, R. van der Schalie, W. Wagner, and W. Dorigo. 2019. "Evolution of the ESA CCI Soil Moisture Climate Data Records and Their Underlying Merging Methodology." *Earth System Science Data* 11 (2): 717–739. <https://doi.org/10.5194/essd-11-717-2019>.
- Gruber, A., C.-H. Su, W. T. Crow, S. Zwieback, W. A. Dorigo, and W. Wagner. 2016. "Estimating Error Cross-Correlations in Soil Moisture Data Sets Using Extended Collocation Analysis." *Journal of Geophysical Research Atmospheres* 121 (3): 1208–1219. <https://doi.org/10.1002/2015JD024027>.
- Hu, F., Z. Wei, X. Yang, W. Xie, Y. Li, C. Cui, B. Yang, C. Tao, W. Zhang, and L. Meng. 2022. "Assessment of SMAP and SMOS Soil Moisture Products Using Triple Collocation Method Over Inner Mongolia." *Journal of Hydrology: Regional Studies* 40:101027. <https://doi.org/10.1016/j.ejrh.2022.101027>.
- Huggannavar, V., and J. Indu. 2020. "Seasonal Variability of Soil Moisture-Precipitation Feedbacks Over India." *Journal of Hydrology* 589:125181. <https://doi.org/10.1016/j.jhydrol.2020.125181>.
- Huszár, T., J. Mika, D. Lóczy, K. Molnár, and Á. Kertész. 1999. "Climate Change and Soil Moisture: A Case Study." *Physics and Chemistry of the Earth, Part A: Solid Earth and Geodesy* 24 (10): 905–912. [https://doi.org/10.1016/S1464-1895\(99\)00134-9](https://doi.org/10.1016/S1464-1895(99)00134-9).
- Jackson, T. J. 1993. "III. Measuring Surface Soil Moisture Using Passive Microwave Remote Sensing." *Hydrological Processes* 7 (2): 139–152. <https://doi.org/10.1002/hyp.3360070205>.
- Jackson, T. J., J. Schmugge, and E. T. Engman. 1996. "Remote Sensing Applications to Hydrology: Soil Moisture." *Hydrological Sciences Journal* 41 (4): 517–530. <https://doi.org/10.1080/02626669609491523>.
- Jones, L. A., J. S. Kimball, E. Podest, K. C. McDonald, S. K. Chan, and E. G. Njoku. (2009, July). A method for deriving land surface moisture, vegetation optical depth, and open water fraction from AMSR-E. In *2009 IEEE International Geoscience and Remote Sensing Symposium*, (Vol. 3, pp. III–916). IEEE.
- Karthikeyan, L., and D. N. Kumar. 2016. "A Novel Approach to Validate Satellite Soil Moisture Retrievals Using Precipitation Data." *Journal of Geophysical Research Atmospheres* 121 (19): 11,516–11,535. <https://doi.org/10.1002/2016JD024829>.
- Kim, S., R. M. Parinussa, Y. Y. Liu, F. M. Johnson, and A. Sharma. 2015. "A Framework for Combining Multiple Soil Moisture Retrievals Based on Maximizing Temporal Correlation." *Geophysical Research Letters* 42 (16): 6662–6670. <https://doi.org/10.1002/2015GL064981>.
- Koike, T., Y. Nakamura, I. Kaihotsu, G. Davaa, N. Matsuura, K. Tamagawa, and H. Fujii. (2004). Development of an advanced microwave scanning radiometer (AMSR-E) algorithm for soil moisture and vegetation water content. *Proceedings Of Hydraulic Engineering*, 48, 217–222.
- Krishnan, S., A. Pradhan, and J. Indu. 2022. "Estimation of High-Resolution Precipitation Using Downscaled Satellite Soil Moisture and SM2RAIN Approach." *Journal of Hydrology* 610:127926. <https://doi.org/10.1016/j.jhydrol.2022.127926>.
- Li, B., M. Rodell, S. Kumar, H. K. Beaudoin, A. Getirana, B. F. Zaitchik, L. G. de Goncalves, et al. 2019. "Global GRACE Data Assimilation for Groundwater and Drought Monitoring: Advances and Challenges." *Water Resources Research* 55 (9): 7564–7586. <https://doi.org/10.1029/2018WR024618>.
- Liu, Y. Y., W. A. Dorigo, R. M. Parinussa, R. A. M. de Jeu, W. Wagner, M. F. McCabe, J. P. Evans, and A. I. J. M. van Dijk. 2012. "Trend-Preserving Blending of Passive and Active Microwave Soil Moisture Retrievals." *Remote Sensing of Environment* 123:280–297. <https://doi.org/10.1016/j.rse.2012.03.014>.

- Ma, H., J. Zeng, N. Chen, X. Zhang, M. H. Cosh, and W. Wang. 2019. "Satellite Surface Soil Moisture from SMAP, SMOS, AMSR2 and ESA CCI: A Comprehensive Assessment Using Global Ground-Based Observations." *Remote Sensing of Environment* 231:111215. <https://doi.org/10.1016/j.rse.2019.111215>.
- Martens, B., D. G. Miralles, H. Lievens, R. van der Schalie, R. A. M. de Jeu, D. Fernández-Prieto, H. E. Beck, W. A. Dorigo, and N. E. C. Verhoest. 2017. "GLEAM V3: Satellite-Based Land Evaporation and Root-Zone Soil Moisture." *Geoscientific Model Development* 10 (5): 1903–1925. [10.5194/gmd-10-1903-2017](https://doi.org/10.5194/gmd-10-1903-2017).
- McColl, K. A., J. Vogelzang, A. G. Konings, D. Entekhabi, M. Piles, and A. Stoffelen. 2014. "Extended Triple Collocation: Estimating Errors and Correlation Coefficients with Respect to an Unknown Target." *Geophysical Research Letters* 41 (17): 6229–6236. <https://doi.org/10.1002/2014GL061322>.
- Miralles, D. G., T. R. H. Holmes, R. A. M. De Jeu, J. H. Gash, A. G. C. A. Meesters, and A. J. Dolman. 2011. "Global Land-Surface Evaporation Estimated from Satellite-Based Observations." *Hydrology and Earth System Sciences* 15 (2): 453–469.
- Njoku, E., T. Jackson, and S. Chan. 2004. "AMSR-E/Aqua Daily L3 Surface Soil Moisture, Interpretive Parameters, & QC EASE-Grids, Version 2 [Dataset]. [object Object]. https://doi.org/10.5067/AMSR-E/AE_LAND3.002.
- Nouri, M., and M. Homaee. 2021. "Contribution of Soil Moisture Variations to High Temperatures Over Different Climatic Regimes." *Soil and Tillage Research* 213:105115. <https://doi.org/10.1016/j.still.2021.105115>.
- ONeill, P. E., S. Chan, E. G. Njoku, T. Jackson, R. Bindlish, M. J. Chaubell, and A. Colliander. 2023. "SMAP Enhanced L3 Radiometer Global and Polar Grid Daily 9 km EASE-Grid Soil Moisture, Version 6 [Dataset]. [object Object]. <https://doi.org/10.5067/M200XIZHY3RJ>.
- Owe, M., R. de Jeu, and J. Walker. 2001. "A Methodology for Surface Soil Moisture and Vegetation Optical Depth Retrieval Using the Microwave Polarization Difference Index." *IEEE Transactions on Geoscience & Remote Sensing* 39 (8): 1643–1654. *IEEE Transactions on Geoscience and Remote Sensing*. <https://doi.org/10.1109/36.942542>.
- Pai, D. S., M. Rajeevan, O. P. Sreejith, B. Mukhopadhyay, and N. S. Satbha. 2014. "Development of a New High Spatial Resolution (0.25° × 0.25°) Long Period (1901–2010) Daily Gridded Rainfall Data Set Over India and Its Comparison With Existing Data Sets Over the Region." *Mausam* 65 (1), Article 1. <https://doi.org/10.54302/mausam.v65i1.851>.
- Pai, D. S., L. Sridhar, M. R. Badwaik, and M. Rajeevan. 2015. "Analysis of the Daily Rainfall Events Over India Using a New Long Period (1901–2010) High Resolution (0.25° × 0.25°) Gridded Rainfall Data Set." *Climate Dynamics* 45 (3–4): 755–776. <https://doi.org/10.1007/s00382-014-2307-1>.
- Peng, J., M. Tanguy, E. L. Robinson, E. Pinnington, J. Evans, R. Ellis, E. Cooper, J. Hannaford, E. Blyth, and S. Dadson. 2021. "Estimation and Evaluation of High-Resolution Soil Moisture from Merged Model and Earth Observation Data in the Great Britain." *Remote Sensing of Environment* 264:112610. <https://doi.org/10.1016/j.rse.2021.112610>.
- Porporato, A., E. Daly, and I. Rodriguez-Iturbe. 2004. "Soil Water Balance and Ecosystem Response to Climate Change." *The American Naturalist* 164 (5): 625–632. <https://doi.org/10.1086/424970>.
- Preimesberger, W., T. Scanlon, C.-H. Su, A. Gruber, and W. Dorigo. 2021. "Homogenization of Structural Breaks in the Global ESA CCI Soil Moisture Multisatellite Climate Data Record." *IEEE Transactions on Geoscience & Remote Sensing* 59 (4): 2845–2862. *IEEE Transactions on Geoscience and Remote Sensing*. <https://doi.org/10.1109/TGRS.2020.3012896>.
- Rao, Y. S., and A. A. Chaudhari. 2009. "Analysis of 7 Years Aqua AMSR-E Derived Soil Moisture Data Over India." 2009 IEEE International Geoscience and Remote Sensing Symposium, III-486–III-489. [10.1109/IGARSS.2009.5418298](https://doi.org/10.1109/IGARSS.2009.5418298).
- Riley, W. J., and C. Shen. 2014. "Characterizing Coarse-Resolution Watershed Soil Moisture Heterogeneity Using Fine-Scale Simulations." *Hydrology and Earth System Sciences* 18 (7): 2463–2483. <https://doi.org/10.5194/hess-18-2463-2014>.
- Rodell, M., P. R. Houser, U. Jambor, J. Gottschalck, K. Mitchell, C.-J. Meng, K. Arsenault, et al. 2004. "The Global Land Data Assimilation System." *Bulletin of the American Meteorological Society* 85 (3), Article 381–394. <https://doi.org/10.1175/BAMS-85-3-381>.

- Rodriguez-Iturbe, I. 2000. "Ecohydrology: A Hydrologic Perspective of Climate-Soil-Vegetation Dynamics." *Water Resources Research* 36 (1): 3–9. <https://doi.org/10.1029/1999WR900210>.
- Rosenbaum, U., H. R. Bogen, M. Herbst, J. A. Huisman, T. J. Peterson, A. Weuthen, A. W. Western, and H. Vereecken. 2012. "Seasonal and Event Dynamics of Spatial Soil Moisture Patterns at the Small Catchment Scale." *Water Resources Research* 48 (10). <https://doi.org/10.1029/2011WR011518>.
- Salvucci, G. D. 2001. "Estimating the Moisture Dependence of Root Zone Water Loss Using Conditionally Averaged Precipitation." *Water Resources Research* 37 (5): 1357–1365. <https://doi.org/10.1029/2000WR900336>.
- Santi, E., S. Paloscia, S. Pettinato, L. Brocca, L. Ciabatta, and D. Entekhabi. 2018. "On the Synergy of SMAP, AMSR2 and Sentinel-1 for Retrieving Soil Moisture." *International Journal of Applied Earth Observation and Geoinformation* 65:114–123. <https://doi.org/10.1016/j.jag.2017.10.010>.
- Schmugge, T. J., T. J. Jackson, and H. L. McKim. 1980. "Survey of Methods for Soil Moisture Determination." *Water Resources Research* 16 (6): 961–979. <https://doi.org/10.1029/WR016i006p00961>.
- Scipal, K., W. Dorigo, and R. DeJeu. 2010. "Triple Collocation—A New Tool to Determine the Error Structure of Global Soil Moisture Products." 2010 IEEE International Geoscience and Remote Sensing Symposium, 4426–4429. <https://doi.org/10.1109/IGARSS.2010.5652128>.
- Scipal, K., T. Holmes, R. de Jeu, V. Naeimi, and W. Wagner. 2008. "A Possible Solution for the Problem of Estimating the Error Structure of Global Soil Moisture Data Sets." *Geophysical Research Letters* 35 (24). <https://doi.org/10.1029/2008GL035599>.
- Shepard, D. (1968, January). A two-dimensional interpolation function for irregularly-spaced data. In *Proceedings of the 1968 23rd ACM national conference*, (pp. 517–524).
- Si, J., J. Li, S. Lu, X. Qi, X. Zhang, W. Bao, X. Zhang, et al. 2023. "Effects of Climate Change on Surface Runoff and Soil Moisture in the Source Region of the Yellow River." *Water* 15 (11), Article 11. <https://doi.org/10.3390/w15112104>.
- Siebert, S., V. Henrich, K. Frenken, and J. Burke. 2013. *Update of the Digital Global Map of Irrigation Areas to Version 5*. 10.13140/2.1.2660.6728.
- Stoffelen, A. 1998. "Toward the True Near-Surface Wind Speed: Error Modeling and Calibration Using Triple Collocation." *Journal of Geophysical Research Oceans* 103 (C4): 7755–7766. <https://doi.org/10.1029/97JC03180>.
- Stoffelen, A. and Vogelzang, J. 2012. "Triple collocation" ResearchGate. <https://doi.org/10.13140/RG.2.2.30926.66888>.
- Sunilkumar, K., T. Narayana Rao, K. Saikranthi, and M. Purnachandra Rao. 2015. "Comprehensive Evaluation of Multisatellite Precipitation Estimates Over India Using Gridded Rainfall Data." *Journal of Geophysical Research Atmospheres* 120 (17): 8987–9005. Scopus. <https://doi.org/10.1002/2015JD023437>.
- Tang, L., Y. Tian, F. Yan, and E. Habib. 2015. "An Improved Procedure for the Validation of Satellite-Based Precipitation Estimates." *Atmospheric Research* 163:61–73. <https://doi.org/10.1016/j.atmosres.2014.12.016>.
- Teng B. & Parinussa R. (2021). Readme Document for LPRM Surface Soil Moisture Data Products.
- Tuttle, S. E., and G. D. Salvucci. 2014. "A New Approach for Validating Satellite Estimates of Soil Moisture Using Large-Scale Precipitation: Comparing AMSR-E Products." *Remote Sensing of Environment* 142:207–222. <https://doi.org/10.1016/j.rse.2013.12.002>.
- Upadhyaya, D. B., J. Evans, S. Muddu, S. K. Tomer, A. Al Bitar, S. Yeggina, S. Thiyaku, et al. 2021. "The Indian COSMOS Network (ICON): Validating L-Band Remote Sensing and Modelled Soil Moisture Data Products." *Remote Sensing* 13 (3), Article 3. <https://doi.org/10.3390/rs13030537>.
- Vogel, M. M., J. Zscheischler, and S. I. Seneviratne. 2018. "Varying Soil Moisture–Atmosphere Feedbacks Explain Divergent Temperature Extremes and Precipitation Projections in Central Europe." *Earth System Dynamics* 9 (3): 1107–1125. <https://doi.org/10.5194/esd-9-1107-2018>.
- Wang, L., Z. Xie, B. Jia, J. Xie, Y. Wang, B. Liu, R. Li, and S. Chen. 2019. "Contributions of Climate Change and Groundwater Extraction to Soil Moisture Trends." *Earth System Dynamics* 10 (3): 599–615. <https://doi.org/10.5194/esd-10-599-2019>.

- Whan, K., J. Zscheischler, R. Orth, M. Shongwe, M. Rahimi, E. O. Asare, and S. I. Seneviratne. 2015. "Impact of Soil Moisture on Extreme Maximum Temperatures in Europe." *Weather and Climate Extremes* 9:57–67. <https://doi.org/10.1016/j.wace.2015.05.001>.
- Wu, Q., H. Liu, L. Wang, and C. Deng. 2016. "Evaluation of AMSR2 Soil Moisture Products Over the Contiguous United States Using *in situ* Data from the International Soil Moisture Network." *International Journal of Applied Earth Observation and Geoinformation* 45:187–199. <https://doi.org/10.1016/j.jag.2015.10.011>.
- Xie, Q., L. Jia, M. Menenti, and G. Hu. 2022. "Global Soil Moisture Data Fusion by Triple Collocation Analysis from 2011 to 2018." *Scientific Data* 9 (1), Article 1. <https://doi.org/10.1038/s41597-022-01772-x>.
- Xu, L., P. Abbaszadeh, H. Moradkhani, N. Chen, and X. Zhang. 2020. "Continental Drought Monitoring Using Satellite Soil Moisture, Data Assimilation and an Integrated Drought Index." *Remote Sensing of Environment* 250:112028. <https://doi.org/10.1016/j.rse.2020.112028>.
- Xu, L., N. Chen, X. Zhang, H. Moradkhani, C. Zhang, and C. Hu. 2021. "In-Situ and Triple-Collocation Based Evaluations of Eight Global Root Zone Soil Moisture Products." *Remote Sensing of Environment* 254:112248. <https://doi.org/10.1016/j.rse.2020.112248>.
- Zhao, H., C. Montzka, H. Vereecken, and H. J. H. Franssen. 2024. "A Comparative Analysis of Remote Sensing Soil Moisture Datasets Fusion Methods: Novel LSTM Approach versus Widely Used Triple Collocation Technique." *IEEE Journal of Selected Topics in Applied Earth Observations & Remote Sensing* 17: 16659–16671.
- Zhou, J., W. T. Crow, Z. Wu, J. Dong, H. He, and H. Feng. 2021. "A Triple Collocation-Based 2D Soil Moisture Merging Methodology Considering Spatial and Temporal Non-stationary Errors." *Remote Sensing of Environment* 263:112509. <https://doi.org/10.1016/j.rse.2021.112509>.
- Zhu, L., H. Wang, C. Tong, W. Liu, and B. Du. 2019. "Evaluation of ESA Active, Passive and Combined Soil Moisture Products Using Upscaled Ground Measurements." *Sensors* 19 (12), Article 12. <https://doi.org/10.3390/s19122718>.
- Zreda, M., W. J. Shuttleworth, X. Zeng, C. Zweck, D. Desilets, T. Franz, and R. Rosolem. 2012. "Cosmos: The Cosmic-Ray Soil Moisture Observing System." *Hydrology and Earth System Sciences* 16 (11): 4079–4099. <https://doi.org/10.5194/hess-16-4079-2012>.